Journal of Alloys and Compounds 543 (2012) 99–104

Contents lists available at SciVerse ScienceDirect

Journal of Alloys and Compounds

journal homepage: www.elsevier.com/locate/jalcom

Synthesis and electrochemical performance of Sn-doped $Li_3V_2(PO_4)_3$/C cathode material for lithium ion battery by microwave solid-state technique

Haiping Liu [a], Sifu Bi [a,*], Guangwu Wen [b], Xiangguo Teng [a], Peng Gao [a], Zujun Ni [a], Yongming Zhu [a], Fang Zhang [a]

[a] School of Marine Science and Technology, Harbin Institute of Technology, Weihai 264209, China
[b] School of Materials Science and Engineering, Harbin Institute of Technology, Weihai 264209, China

ARTICLE INFO

Article history:
Received 4 June 2012
Received in revised form 15 July 2012
Accepted 16 July 2012
Available online 24 July 2012

Keywords:
Cathode material
Lithium vanadium phosphate
Sn doping
Microwave
Lithium-ion battery

ABSTRACT

$Li_3V_{2-x}Sn_x(PO_4)_3$/C cathode materials with uniform and fine particle sizes were successfully and fast synthesized by a microwave solid-state synthesis method. X-ray diffraction patterns demonstrated that the appropriate addition of Sn did not destroy the lattice structure of $Li_3V_2(PO_4)_3$/C, but decreased the unit cell volume. X-ray photoelectron spectroscopy analysis demonstrated that the main chemical state of V in the $Li_3V_{1.95}Sn_{0.05}(PO_4)_3$/C composite is +3 valence, while the chemical state of Sn in the $Li_3V_{1.95}Sn_{0.05}(PO_4)_3$/C is +4 valence. Scanning electron microscope analysis illustrated that the addition of Sn slightly affected the morphology of samples. As the cathode materials for Li-ion batteries, $Li_3V_{2-x}Sn_x(PO_4)_3$/C ($x \leqslant 0.10$) exhibited higher discharge capacity and better cycle stability than the pure one. At a discharge rate of 0.5 C in the potential range of 2.5–4.5 V at room temperature, the initial discharge capacity of $Li_3V_{1.95}Sn_{0.05}(PO_4)_3$/C was 136 mA h/g. The low charge-transfer resistances and large lithium ion diffusion coefficients confirmed that Sn-doped $Li_3V_2(PO_4)_3$/C samples possessed better electronic conductivity and lithium ion mobility. These improved electrochemical performances can be attributed to the appropriate amount of Sn doping in $Li_3V_2(PO_4)_3$/C system by enhancing structural stability and electrical conductivity. The present study also demonstrates that the microwave processing is a fast, simple and useful method for the fabrication of $Li_3V_2(PO_4)_3$/C crystals.

1. Introduction

Lithium-ion secondary battery, with its large energy density, higher output power and better safety performance, has been already proposed as potential energy source for electric vehicles (EVs) and hybrid electric vehicles (HEVs). Recently, lithium transition metal phosphates, such as $LiFePO_4$, $LiMnPO_4$, $LiCoPO_4$ and $Li_3V_2(PO_4)_3$ [1–6], has been considered as promising cathode materials for lithium-ion batteries. Compared with other lithium transition metal phosphates, monoclinic $Li_3V_2(PO_4)_3$ provides excellent electrochemical performances such as the highest theoretical specific capacity of 197 mA h/g, high-potentials of 3.60, 3.65, 4.10 V (for V^{4+}/V^{3+}) and 4.55 V (for V^{5+}/V^{4+}) [7,8]. Moreover, the Li^+ diffusion coefficient in $Li_3V_2(PO_4)_3$ ranged from 10^{-9} to 10^{-10} cm^2 s^{-1}, which is much higher than that in $LiFePO_4$ ($D_{Li+} = 10^{-14}$–10^{-15} cm^2 s^{-1}) [9,10]. These features indicate that $Li_3V_2(PO_4)_3$ is a most promising cathode material for lithium-ion batteries.

However, the low electronic conductivity of $Li_3V_2(PO_4)_3$ degrades its electrochemical performance and hinders practical application. Some improvements on the electrochemical performance of $Li_3V_2(PO_4)_3$ have been achieved by using carbon coating [11–16], metal oxide coated [17] or metal cation doping [18], such as Nb^{5+}, Zr^{4+}, Ti^{4+}, Fe^{3+}, Cr^{3+}, Co^{2+}, Al^{3+}, Y^{3+}, Mn^{2+}, Mg^{2+} and Ce^{3+} in vanadium sites in $Li_3V_2(PO_4)_3$ systems [19–29].

All these doped metal cations influence the electrical conductivity and enhance cycle properties of $Li_3V_2(PO_4)_3$ to different extents. However, the doping of some metals sacrifices of discharge specific capacity. Sn doping has been shown to be favorable in $LiNi_{0.8}Co_{0.2}O_2$ [30], $LiFe_{1-x}Sn_xPO_4$/C [31], nanosized α-MnO_2 [32], $Li_{3.9}Sn_{0.1}Ti_5O_{12}$ [33] and other Li-based materials. To our knowledge, no studies relating to tin doping in $Li_3V_2(PO_4)_3$ have yet been reported.

$Li_3V_2(PO_4)_3$ had already been prepared by using conventional solid-state synthesis methods [34–36]. However, the conventional solid-state synthesis processes need high calcinations temperature and long reaction time. Microwave solid-state synthesis method as a novel method has been developed to prepare cathode materials for lithium batteries for its uniform and rapid heating with several minutes [37,38]. In this paper, the single-phase Sn-doped $Li_3V_2(PO_4)_3$/C samples have been synthesized in 15 min by using microwave solid-state synthesis. The effects of Sn^{4+} doping on the structure and electrochemical properties are also discussed in details.

* Corresponding author. Tel./fax: +86 631 5687232.
E-mail address: bisifu@126.com (S. Bi).

0925-8388/$ - see front matter © 2012 Elsevier B.V. All rights reserved.
http://dx.doi.org/10.1016/j.jallcom.2012.07.077

2. Experimental

The $Li_3V_{2-x}Sn_x(PO_4)_3$/C (x = 0, 0.01, 0.02, 0.05 and 0.10) compounds were all prepared using a microwave solid state method. The analytical reagents $LiOH{\cdot}H_2O$, V_2O_5, $NH_4H_2PO_4$, SnO_2 and sucrose were stoichiometrically blended together. The mixture was ball-milled for 3 h in an alcohol medium, and then first heated to 80 °C for 4 h in a vacuum drying oven to evaporate the alcohol and water. Then the mixture was put in a furnace with a flowing argon atmosphere and preheated at 300 °C for 3 h to get precursor. Finally, the precursor was put into the self-designed reactor in which graphite was used as the microwave absorber and the reducing agent. The microwave heating lasted 15 min at 750 °C in a microwave oven.

The phase identification of the $Li_3V_{2-x}Sn_x(PO_4)_3$/C samples was carried out using X-ray powder diffraction (XRD). The diffraction intensity data were collected using a DX2700 diffractometer with Cu Ka radiation (DanDong Haoyuan, China). The morphology of the samples was observed on a scanning electron microscope (Quanta 200, America). X-ray photoelectron spectroscopy (XPS) (PHI5700, America) with monochromatic Al Kα radiation was employed to investigate the oxidation state of V and Sn in the $Li_3V_{2-x}Sn_x(PO_4)_3$/C samples. The binding energy values were calibrated by using the value of contaminant carbon (C1s = 284.6 eV) as a reference.

The electrochemical properties of $Li_3V_{2-x}Sn_x(PO_4)_3$/C powders as cathodes in the two-electrode electrochemical cells were evaluated in an automatic battery testing system (Land, China). The cathodes of the two-electrode electrochemical cells were fabricated by blending the prepared powder with acetylene black and a polyvinylidene fluoride (PVDF) binder at a weight ratio of 80:10:10 in N-methyl-2-pyrrolidine (NMP). The obtained slurry was coated on Al foil, dried at 80 °C for 2 h and pressed at a pressure of 5 MPa. The fabricated electrodes were dried again at 120 °C for 4 h in vacuum and cut into circles with diameter 15 mm in size. The two-electrode electrochemical cells were assembled in a glove box (Universal 2440/750, Mikrouna) filled with high-purity argon, using a polypropylene membrane (Celgard 2400) as the separator, lithium metal foil as the anode, and 1M LiPF6 in EC:DMC (1:1, vol.%) as the electrolyte. The electrochemical capacity measurements were performed in the voltage range between 2.5 and 4.5 V vs. Li/Li^+ at 0.5 C rate based on the weight of $Li_3V_2(PO_4)_3$/C (1C = 132 mA h/g), and the electrochemical capacities of the samples were evaluated for the active materials.

3. Results and discussion

The XRD patterns of $Li_3V_{2-x}Sn_x(PO_4)_3$/C (x = 0, 0.01, 0.02, 0.05 and 0.10) compounds are shown in Fig. 1. All the samples were found to be single-phase and no impurity phases can be detected within the resolution of our diffractometer. The whole diffraction peaks positions have some right shift with the x value increased, especially in large angle region. The X-ray diffraction patterns of $Li_3V_{2-x}Sn_x(PO_4)_3$/C compounds were successfully indexed with a monoclinic lattice using the program Dicvol.

The unit cell lattice parameters of all the experimental $Li_3V_{2-x}Sn_x(PO_4)_3$ phases are summarized in Table 1. It can be seen that, after Sn doping, the lattice constant a-axis firstly decreases, and then slightly increases ($x \geqslant 0.05$); while the lattice constants b- and c-axis decrease with increasing the Sn content. These changes give rise to a decrease of the unit cell volume. When x changes in the range of 0 and 0.05, the decrease of the lattice constants is due to the difference of ionic radius where the radius of Sn^{4+} (0.55 Å) ion is smaller than that of V^{3+} (0.64 Å) ion [39]. In addition, considering the valences of tin and vanadium cations

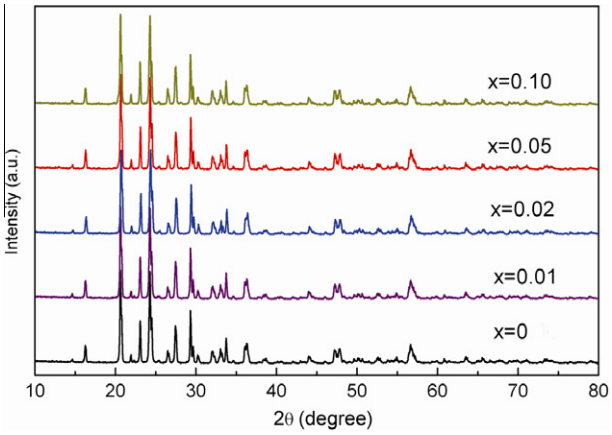

Fig. 1. X-ray diffraction profiles of $Li_3V_{2-x}Sn_x(PO_4)_3$/C with different tin contents (x = 0, 0.01, 0.02, 0.05 and 0.10).

Table 1
Refined unit cell lattice parameters for $Li_3V_{2-x}Sn_x(PO_4)_3$/C cells (x = 0, 0.01, 0.02, 0.05, 0.10).

x	a (Å)	b (Å)	c (Å)	B (°)	V (Å^3)
0	8.591734	8.603524	12.03256	90.35902	889.42
0.01	8.548356	8.605193	12.03117	89.48702	884.98
0.02	8.580146	8.58393	12.02138	90.40112	885.37
0.05	8.605336	8.585531	11.97608	90.31426	884.8
0.10	8.609417	8.596206	11.99715	90.23327	887.88

are +4 and +3, respectively, the substitution of V^{3+} by Sn^{4+} will demand a charge compensation mechanism to achieve electrical neutrality. Thus, replacing V^{3+} with Sn^{4+} will lead to the formation of V^{2+}. The radius of V^{2+} (0.79 Å) is larger than that of V^{3+} (0.64 Å). And thus, when x = 0.10, due to this un-equivalent substitution, it may introduce more V^{2+} and cause the unit cell volume increase slightly than that of x = 0.05.

Fig. 2 shows the XPS result of Sn-doped $Li_3V_2(PO_4)_3$/C material. Fig. 2(a) depicts the V 2p XPS core level for the as-prepared $Li_3V_{1.95}Sn_{0.05}(PO_4)_3$/C composite. The V 2p core level fits to a single peak with a binding energy of 516.87 eV, demonstrating that the main chemical state of V in the $Li_3V_{1.95}Sn_{0.05}(PO_4)_3$/C composite is +3 valence according to the literature [40–42]. The XPS peak position of Sn 3d is about 487.16 eV (Fig. 2(b)), matching well with the data of Sn^{4+} in Sn-doped materials reported in literature [30,31].

The SEM images of the $Li_3V_{2-x}Sn_x(PO_4)_3$/C (x = 0, 0.01, 0.02, 0.05 and 0.10) compounds are shown in Fig. 3. As seen in Fig. 3, a particles size of 0.1–3 μm and aggregated structure can be seen for $Li_3V_2(PO_4)_3$/C sample (Fig. 2(a)), while the Sn doping samples have a smaller particles size and narrower particles size distribution (Fig. 3((b)–(e)). These results confirm that the addition of Sn may slightly affect the morphology of samples. The small particle size results in sufficient contact between active materials and electrolyte, which is favorable for the diffusion and transmission of Li^+ in the electrode [43].

Electrochemical impedance spectroscopy (EIS) measurements were used to investigate the electrochemical dynamic behavior of $Li_3V_{2-x}Sn_x(PO_4)_3$/C (x = 0, 0.05) materials. Fig. 4 shows the corresponding Nyquist plots and the inset is the equivalent circuit used to fit the EIS. A semicircle was observed to center on the real axis at the high frequency range. In the low frequency range, a straight line corresponds to the Warburg impedance. The high frequency semicircle is related to the charge-transfer resistance (R_{ct}) and the double-layer capacitance, while the low frequency tails re-